https://doi.org/10.5194/egusphere-2026-7101
Preprint. Discussion started: 20 November 2026
© Author(s) 2026. CC BY 4.0 License.

Identifying new particle formation events by using a simple and low-cost diffusion charger monitor

Ashkan Jahandari[1], Rohan Jayaratne[1], Alícia Josa-Culleré[1], Lidia Morawska[1]*

[1]International Laboratory for Air quality and Health (ILAQH), School of Earth and Atmospheric Sciences, Queensland University of Technology, Brisbane, Queensland 4001, Australia

Correspondence: Lidia Morawska, International Laboratory for Air quality and Health (ILAQH), School of Earth and Atmospheric Sciences, Queensland University of Technology, Brisbane, Queensland 4001, Australia. l.morawska@qut.edu.au

Abstract. New particle formation (NPF) is a major source of ultrafine particles (UFPs) in the atmosphere and plays an important role in air quality and human health. NPF events are usually identified from particle number size distribution measured with complex instruments such as the scanning mobility particle sizer (SMPS) and the Neutral cluster and Air Ion Spectrometer (NAIS). The Naneos Partector2 Pro (P2Pro) measures particle number concentrations (PNC) in eight size bins between 7.8 and 382.4 nm using a unipolar diffusion charger. This study investigated whether this simple and lower-cost instrument can be used for detecting NPF events with performance comparable to reference instruments. To do this, we monitored PNC in Brisbane using a P2Pro over a year. A method was developed and validated by comparing the results with previous studies reported in the same area using the NAIS or SMPS. The analysis was carried out under various combinations of three main sets of criteria – the total PNC, the fraction of particles in the nucleation mode, and the times of occurrence of the events. The results, based on the selected criteria showed that NPF events occurred on 158 (44 %) days of the year. The results showed excellent agreement with previous estimates of NPF events at the same location obtained using an SMPS and NAIS. The outcome of this study offers an affordable alternative to an instrument that can detect NPF events that are important in many aspects such as air quality monitoring and health risk assessment.

1 Introduction

Atmospheric aerosols include primary and secondary particles. Primary particles are emitted directly into the air by combustion processes such as traffic emissions or cooking, whereas secondary particles are formed through atmospheric gas-to-particle conversion processes (Kalkavouras et al., 2024; Vu et al., 2015). These processes include binary nucleation (H_2SO_4-H_2O), ternary nucleation (H_2SO_4-H_2O-NH_3), and ion-induced nucleation involving charged particles (Holmes, 2007). After nucleation, particles subsequently grow through condensation and coagulation (Zhang et al., 2012). This sequence of processes, known as new particle formation (NPF), constitutes a major source of ultrafine particles (UFPs; particles smaller than 100 nm in diameter) in the atmosphere (Lehtipalo et al., 2025). Due to their small size, UFPs contribute little to the particle mass.

https://doi.org/10.5194/egusphere-2026-7101
Preprint. Discussion started: 20 November 2026
© Author(s) 2026. CC BY 4.0 License.

However, they contribute importantly to the particle number concentration (PNC), another metric to characterize the submicron aerosol. UFPs typically account for around 80 % of PNC. Studies suggest that NPF can contribute up to 60–90 % of PNC in urban areas and other environments (Lee et al., 2024; Ristovski et al., 2010; Ueda et al., 2016; Venzac et al., 2008), highlighting the importance of secondary particles in shaping urban air quality (Kulmala, 2025).

Improving air quality based only on mass-based metrics does not guarantee reductions in UFP levels (De Jesus et al., 2019). Although UFPs have adverse effects on respiratory and cardiovascular health (Delfino et al., 2005; Lachowicz and Gać, 2025; Schraufnagel, 2020), UFP are not yet regulated. The World Health Organization (WHO) has recognized UFPs as a public health concern but noted that current evidence is insufficient to establish guideline values (Who, 2021). Addressing this gap requires better quantification of UFP sources, which influence the size and composition of particles (Vu et al., 2015). Furthermore, because primary and secondary particles differ in composition and potential health effects, distinguishing between them is crucial for health risk assessment and the development of UFP air quality guidelines.

This, however, presents two challenges: first, how to monitor UFPs to obtain particle number size distribution (PNSD), and second, how to identify NPF events from the monitoring results. These two challenges are not independent, because the identification of NPF depends on how the particles are measured. PNSD is commonly measured with scanning mobility particle sizer (SMPS) or a neutral cluster and air spectrometer (NAIS). These instruments differ in measurement principle, detection limit, and particle size range. The lower detection limit is important for NPF identification because the initial steps of NPF occur below 10 nm. The NAIS, with a detection limit of 1–2 nm and size range up to 40 nm, provides data on the early stages of nucleation and particle formation rates. In contrast, SMPS systems measure a wider size range (10–900 nm), making them a suitable option for evaluating and quantifying subsequent particle growth. Pushpawela et al. (2018a) showed that particle growth can be mistakenly classified as an NPF event when an instrument cannot detect very small particles, as such an instrument may fail to detect the rapid increase in PNC below 30 nm that is a key sign of nucleation (Kulmala et al., 2004).

NPF begins when precursor gases form new clusters that grow into the nucleation mode. NPF most likely occurs when photochemical production of sulfuric acid from SO_2 peaks around midday and the concentration of pre-existing particles is low so that condensable species are not scavenged. In the size distribution data, this appears as a sudden increase in the number of particles in the nucleation mode range, followed by growth over several hours. At present, several approaches are used to identify NPF events. The method proposed by Dal Maso et al. (2005) is mostly used, in which each day is classified as an event, a non-event or undefined, based on a sudden increase in PNC and the appearance of nucleation mode particles followed by particle growth. Lehtipalo et al. (2025) noted that most studies still use this method or a revised version of it (e.g., Buenrostro Mazon et al. (2009)) and because this method relies on visual inspection of PNSD data, such as the characteristics of banana shape, the results can be subjective and are affected by the experience of the classifier. Source apportionment using positive matrix factorization (PMF) is another way to identify and apportion UFP sources, including photochemically nucleated particles. PMF is a multivariate factor analysis that combines PNSD data with chemical and meteorological information to estimate the contribution of different source profiles (Garcia-Marlès et al., 2024b). Detailed information about PMF is discussed by Vu et al. (2015). More advanced statistical and data science methods have also been developed, including

https://doi.org/10.5194/egusphere-2026-7101
Preprint. Discussion started: 20 November 2026
© Author(s) 2026. CC BY 4.0 License.

automatic search algorithms based on PNSD parameters, nanoparticle ranking analysis, and advanced machine learning algorithms (Lehtipalo et al., 2025and reference therein). Despite promising results, Lehtipalo et al. (2025) concluded that no universal automated method independent of site and instrument exists yet, because pre-existing particle size distribution and instrument capabilities vary across locations. Table 1 gives an overview of some common methods used for identified NPF events.

Table 1. Methods used in the literature for NPF identification

Study	Environment	Instrument	Size Range	Nucleation/ PNC thresholds	Duration
Covert et al. (1992)	Marine	DMA/ CPC	20–600 nm	(N_{total}- N_{15}/N_{15})> 50 %	~ 2 h
Mäkelä et al. (1997)	Forest	DMA/ CPC	3 -500 nm	N_{nuc}/(N_{Aitken}+N_{acc})	3-4 h
Birmili and Wiedensohler (2000)	Grassland	DMPS/CPC	3 - ~600 nm	PNC > 10^4 cm^{-3}	4 h
Stanier et al. (2004)	Urban	DMA/CPC	3– 680 nm	N_{10}> ~10^4 cm^{-3}	~ 1h
Dal Maso et al. (2005)	Forest	DMA/CPC	3–1000 nm	Appearance of a distinct new mode in the nucleation range	Several hours
Guo et al. (2008)	Urban	EC/CPC	15 – 737 nm	Clear increase in N_{nuc} concentration	Several hours
Mejía and Morawska (2009)	Urban	EC/CPC	14– 800 nm	The concentration of N_{14-30}> 50%[h]	1 hour and more
Buenrostro Mazon et al. (2009)	Forest	DMA/CPC	3– 500 nm	Redefine Dal Maso et al. (2005), Distinct mode <25 nm	> 1 h
Jayaratne et al. (2016)	Urban	NAIS	0.8-42 nm	N_{10}> 1.5×10^3 cm^{-3} dN/dt> 1.5×10^3 cm^{-3} h^{-1}	1 hour and more
Salimi et al. (2017)	Urban	SMPS	9-414 nm	Dal Maso et al. (2005) method	Several hours
Pushpawela et al.(2018a,b)	Urban	NAIS	0.8-42 nm	N_{2-10}>10^4 cm^{-3} dN/dt> 10^4 cm^{-3} h^{-1}	1 hour and more

Differential Mobility Analyzer (DMA); Condensation Particle Counter (CPC); N_{total}: the total particle number concentration (PNC), N_{15}: particles with a diameter larger than 15 nm; N_{nuc}: the PNC of nucleation mode, N_{Aitken}: the PNC of Aitken mode, N_{acc}: the PNC of accumulation mode; Differential Mobility Particle Sizer (DMPS); N_{10}: the PNC of particles with a diameter between 3-10 nm; Electrostatic Classifier (EC); and N_{14-30}: particles with a diameter between 14 nm and 30 nm.

As mentioned above, the criteria for identifying NPF events depend on the instruments used (Lehtipalo et al., 2025; Pushpawela et al., 2018a). Instruments used for NPF identification are complex and require regular calibration, maintenance, and trained

https://doi.org/10.5194/egusphere-2026-7101
Preprint. Discussion started: 20 November 2026
© Author(s) 2026. CC BY 4.0 License.

operators, which limits long-term measurements and large-scale deployment. Therefore, a better understanding of NPF events and their role in air quality requires an affordable, portable, and user-friendly instrument. The Partector2 Pro (P2Pro) is a portable unipolar diffusion charger that measures eight size channels between 10 and 300 nm, but it has not previously been used to identifying NPF. This study evaluates whether NPF events can be identified using the P2Pro at an urban site by (i) developing and testing a method and (ii) comparing the resulting NPF event frequency with that from pervious NAIS measurement at the same location.

2 Methods

We conducted a longitudinal study with 12 months of continuous PNC and PNSD measurement, as part of the global project "Ultrafine Particle Monitoring to Support WHO 2021 UFP Good Practice". This project aims to assess whether the P2Pro can perform comparably to reference instruments for monitoring UFPs.

2.1 Monitoring site

Data were collected continuously from November 2024 to October 2025 at the International Laboratory for Air Quality and Health (ILAQH) of the Queensland University of Technology (QUT), on the roof of P Block building at the Gardens Point campus in Brisbane, Australia. The site lies within the Central Business District (CBD), on the edge of the City Botanic Gardens and Brisbane River, and about 100 m from the Pacific Motorway which runs along the south-western side of the campus. Air pollution sources at the study site depend on wind direction. The QUT Gardens Point campus lies south-east of the city centre, approximately 100 m from the Southeast Freeway (M3 Pacific Motorway), which runs along the south-western side of the campus (Cheung et al., 2011; Phunthirawuthi et al., 2026). Pollutants associated with north-easterly winds can be attributed to industrial emissions from Brisbane Airport, an oil refinery, and the Port of Brisbane, while those associated with winds from the south through to the north-west reflect local traffic (Cheung et al., 2011).

2.2 Instrumentation

The P2Pro (naneos, Switzerland) operates on the principle of unipolar diffusion charging combined with induced current measurement (Fierz et al., 2014; Naneos, 2026). The instrument determines PNC and size of the particles based on the electrical current by the charged particles. In brief, air is first drawn into the device and passes through a corona charger, which charges the particles. The charged particles then pass through two electrometers separated by an electrostatic precipitator. The first electrometer measures the current of all charged particles, and the second measures the current of the remaining charged particles after the precipitator removes particles above a mobility cut-off set by the deposition voltage (Fierz et al., 2014). By applying four different voltages, the instrument determines the PNSD across eight size channels ranging from 10 nm to 300 nm (Bischof et al., 2026; Maes et al., 2025; Naneos, 2026).

https://doi.org/10.5194/egusphere-2026-7101
Preprint. Discussion started: 20 November 2026
© Author(s) 2026. CC BY 4.0 License.

2.3 Data analysis

The instrument was set to a temporal resolution of 16 s, resulting in an effective measurement interval of 18 s (Naneos, 2026). Data analysis and visualization were carried out using Excel and R statistical software. We measured PNC for 365 days. After excluding four days without complete 24 h measurements, 361 days were included in the analysis.

2.4 NPF event identification

An NPF event is characterized by a sudden burst of newly formed nucleation-mode particles (i.e. <30 nm), a rapid increase in total PNC over a short time, and subsequent growth of particles to larger modes under favourable atmospheric conditions, as described by Lehtipalo et al. (2025and reference therein). Because the P2Pro has only eight size channels between 10 and 300 nm, previous methods could not be applied directly to its data, so criteria appropriate to the instrument were developed instead. For NPF identification in this study, the first two size channels, with mean diameters of 10 and 16.26 nm (ranging from 7.8 to 20.7 nm), were classified as the nucleation mode, while the sum of all eight channels represented the total PNC.
Based on the previous evidence (Table 1), we identified a potential event when (1) the 30-minute average total PNC exceeded a specific threshold, (2) the ratio of nucleation-mode particle concentration to total PNC was above 50 %, and (3) the event was separated by at least 3 h from the previous event.

A sensitivity analysis was used to select the total PNC threshold required for a period to be considered as a candidate NPF event when the nucleation mode particles contributed more than 50 % of the total concentration (Mejía and Morawska, 2009; Peng et al., 2017). Following Dal Maso et al. (2005), some studies used a specific PNC as an indicator of nucleation bursts, while others identified events by assessing of PNSD such as the characteristic banana shape. Birmili and Wiedensohler (2000) used a threshold of 1.0×10^4 cm^{-3} for total PNC. Stanier et al. (2004) and Pushpawela et al. (2018a) used a threshold of 1.0×10^4 cm^{-3} for particles in the 3-10 nm and 2-10 nm, respectively. In an automated method presented by Dada et al. (2018), a threshold of seven times the background concentrations (00:00 to 04:00) was used to identify NPF events. This scaling factor was chosen to reproduce their own manual classification at the same site. Because NPF identification depends on the instrument used, a threshold derived for one instrument cannot be applied to another with a different detection limit and size range. Therefore, the threshold in this study was selected by comparing the event frequency it produced with frequencies reported for the same site using an NAIS as the reference instrument for NPF identification.
In this study, five candidate PNC thresholds were tested: 1.0×10^4 cm^{-3}, 1.5×10^4 cm^{-3}, 2.0×10^4 cm^{-3}, 2.5×10^4 cm^{-3}, and 3.0×10^4 cm^{-3}. The resulting variation in event frequency was compared with previous studies. This approach was used to determine an appropriate threshold for nucleation bursts that captures weak events while avoiding the misclassification of primary particles. It was also used to ensure that the NPF frequencies derived from the P2Pro were comparable to the earlier results in the study area. More details on the threshold selection are provided in the following section, and the results and the selected threshold

https://doi.org/10.5194/egusphere-2026-7101
Preprint. Discussion started: 20 November 2026
© Author(s) 2026. CC BY 4.0 License.

are given in Sec 3.1. Finally, NPF events were further evaluated by examining the time series of PNC and particle size to verify whether each event was correctly identified. The suggested NPF decision tree for the P2Pro is shown in Fig. 1.

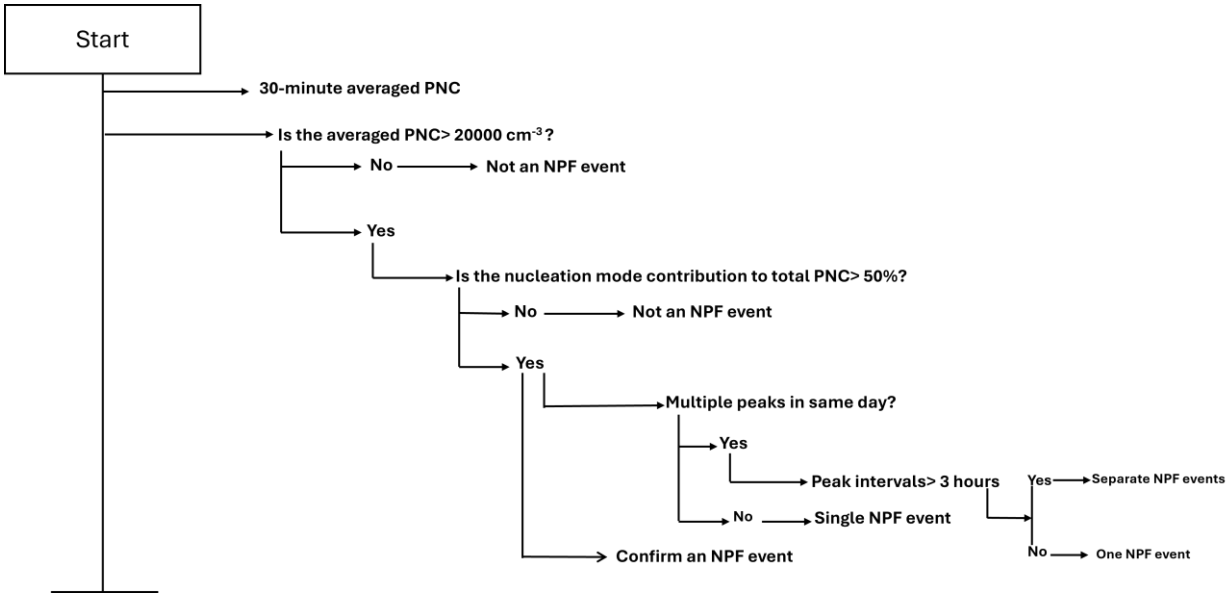


Figure 1. Flow chart illustrating the method for identifying NPF events using P2Pro instrument

3 Results and discussion

3.1 Selection of the total PNC

The NPF event frequencies obtained with the candidate thresholds ranged from 26 % to 77 % (Fig. 2). NPF frequencies previously reported in Brisbane range from 26 % to 67 % (Table 2). However, these studies were conducted at different locations and with different instrument, methods, and campaign durations, so not all of them can be compared directly with our data set. Guo et al. (2008) reported 35 % over 22 days in September at a site 35 km south-east of Brisbane, in the month with the highest sunlight hours and lowest rainfall, conditions that favour photochemical nucleation. Applying candidate thresholds of 3×10^4 and 2.5×10^4 cm^{-3} gave the frequencies of 23 % and 32 %, respectively. The frequency from a short campaign under the favourable conditions for NPF is not likely to be representative of the annual frequency. Similarly, Mejía and Morawska (2009) reported 26 % over 56 non-consecutive days at a site 22 km north-east of the CBD. These results cannot be compared directly with our data set, collected continuously over 12 months. These two candidate thresholds likely capture only strong NPF events; therefore, we did not consider them in our comparison. In contrast, lower thresholds may be too sensitive, potentially classifying primary particles as nucleation events. For example, the 1×10^4 cm^{-3} and 1.5×10^4 cm^{-3}

https://doi.org/10.5194/egusphere-2026-7101
Preprint. Discussion started: 20 November 2026
© Author(s) 2026. CC BY 4.0 License.

thresholds produced frequencies of 78 % and 61 %, respectively. Salimi et al. (2017) reported 67 % from 285 days measurement between 2010 and 2012, with two consecutive weeks of measurement at each of 25 locations across the Brisbane. Because these measurements were not continuous at a single site, these results were not used in selecting the threshold.

Among these studies, only the NAIS measurements were conducted continuously at the same location. These studies reported NPF frequencies between 37 % and 45 %. The 2×10^4 cm^{-3} candidate threshold gave a frequency of 44 % (158 NPF days over 361 days), which is very close to the frequencies from previous NAIS studies (Fig. 2). It should be noted that the measurement of Pushpawela et al. (2018a) and Pushpawela et al. (2018b) were conducted over several years. Only the measurement of Jayaratne et al. (2016) covered a calendar year. Despite the differences in monitoring duration, the frequencies reported by these studies are close. Therefore, the 2×10^4 cm^{-3} threshold was selected and used for all further analysis.

Table 2. Summary of previous NPF studies conducted in the Brisbane region compared with present study

Observation date	Observation site	Instruments	Duration of measurements	Event frequency	References
September 2006	35 km SE of CBD	SMPS	22 days	35 %	(Guo et al., 2008)
May 2006-2007	20 km NE of CBD	SMPS	56 days	26 %	(Mejía and Morawska, 2009)
October 2008- August 2012	Brisbane urban area	SMPS	285 days	67 %	(Salimi et al., 2017)
2012 calendar year	Gardens Point campus, QUT, Brisbane	NAIS	241 days	45 %	(Jayaratne et al., 2016)
Between 2012-2017	Gardens Point campus, QUT, Brisbane	NAIS	485 days	37 %	(Pushpawela et al., 2018a)
Between 2015-2018	Gardens Point campus, QUT, Brisbane	NAIS	232 days	41 %	(Pushpawela et al., 2018b)
July 2022-March 2023	Gardens Point campus, QUT, Brisbane	SEMS[a]	215 days	26 %	(Morawska et al., 2023)
November 2024- October 2025	Gardens Point campus, QUT, Brisbane	Partector2 Pro	361 days	43 %	This study

[a] Scanning Electrical Mobility Spectrometer (SEMS)

It is worth noting that the NAIS studies were conducted several years ago, and some changes might be expected. For example, long-term observations in European cities indicated that, although Aitken and accumulation modes concentrations decreased

https://doi.org/10.5194/egusphere-2026-7101
Preprint. Discussion started: 20 November 2026
© Author(s) 2026. CC BY 4.0 License.

over a decade because of air quality policies, changes in nucleation-mode particles were inconsistent, and in some cases an increase was reported (Garcia-Marlès et al., 2024b, 2024a). This has been linked to the lower condensation sink, rising temperatures, and the low efficiency of diesel particulate filters in capturing semi-volatile organic compounds that contribute to the particle formation (Garcia-Marlès et al., 2024a). A similar decline of 46 % in the Aitken mode concentrations has been reported over the long-term in Brisbane (Phunthirawuthi et al., 2026). However, this study included only the Aitken mode (25–100 nm), so its findings cannot be extended to the nucleation mode. Nevertheless, Morawska et al. (2023) and Phunthirawuthi et al. (2026) noted that the sulfur content of fuel in Australia decreased from 500 ppm before 2006 to 10 ppm at present; as a result, the concentration of SO_2, reported to be the main precursor gas in Brisbane, has decreased. At the same time, lower primary particles emissions resulting from vehicle emission standards and policies such as low-cost public transport have reduced the condensation sinks. These opposing effects could offset each other, leading to a relatively stable NPF frequency in Brisbane; therefore, the results of the NAIS studies remain valid for comparison in this study. It should be noted that the comparison is based on the event frequency rather than the identification criteria, because the criteria differ among instruments and are not directly comparable.

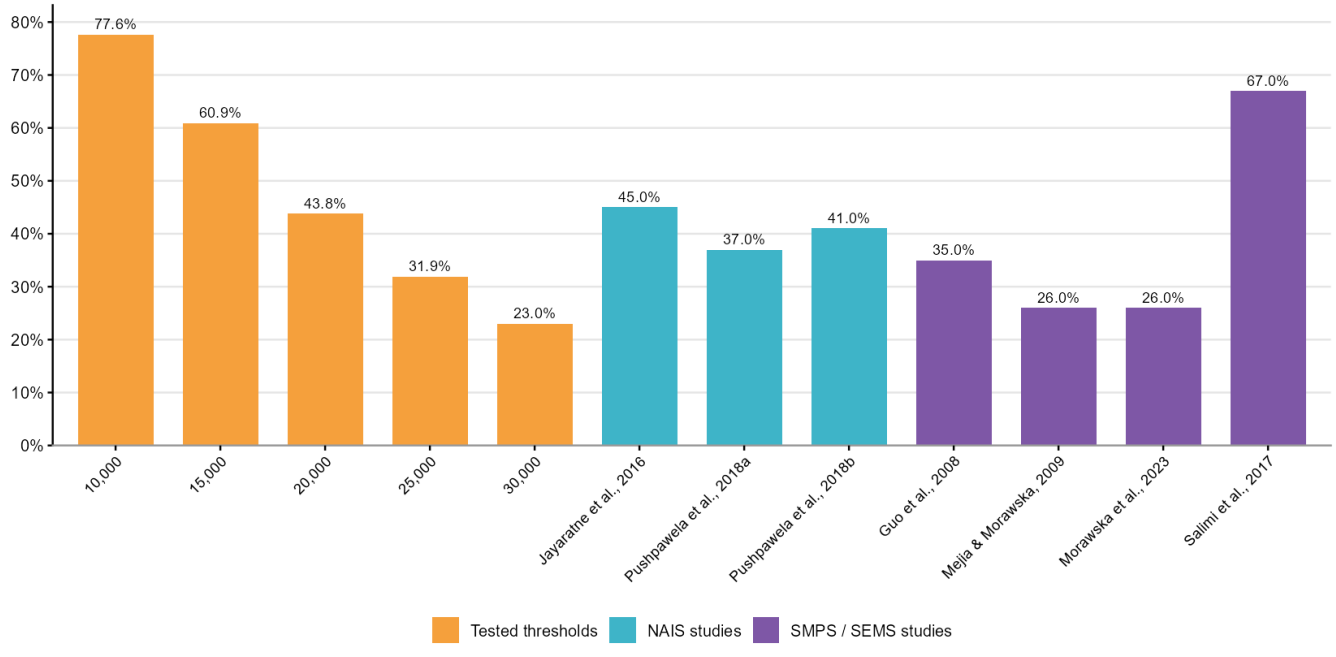


Figure 2. Comparison of potential NPF event frequencies with different PNC thresholds with earlier event frequencies in Brisbane conducted by different instrument.

https://doi.org/10.5194/egusphere-2026-7101
Preprint. Discussion started: 20 November 2026
© Author(s) 2026. CC BY 4.0 License.

With this threshold, 174 events were identified across 158 event days (44 %), with an average of one event day every 2.3 days (Fig. 3). Most events were single-event days (142 days), while the remaining 16 days had two events each. No significant variation was observed, and the frequency of detected events decreasing as follows: winter (49 %) > spring (48 %) > summer (42 %)> autumn (35 %). More specifically, August showed the highest frequency (64 %) and February the lowest (25 %) (Fig. 4). Events were most frequent around midday, with peak PNC occurring between 11:00 and 13:00 local time (LT) in over half of all events (55 % combined), consistent with nucleation-mode PNC in the 10:00-12:00 time window being higher than the concentration on non-event days (4.3×10^3 cm^{-3}). The mean total PNC values for event and non-event days were 1.2×10^4 and 8.0×10^3 cm^{-3}, respectively, representing a 52 % increase in total PNC. This increase was driven by nucleation-mode particles, which increased approximately 2-fold, from 2.83×10^3 cm^{-3} to 5.6×10^3 cm^{-3}. Guo et al. (2008), describing a typical NPF event in Brisbane measured with an SMPS, reported nucleation-mode particle concentrations of about 5.68×10^3 cm^{-3} at noon. In addition, the contribution of this mode to total PNC increased from 36 % on non-event days to 40 % during event days, highlighting the dominant role of secondary particles in total PNC on event days.

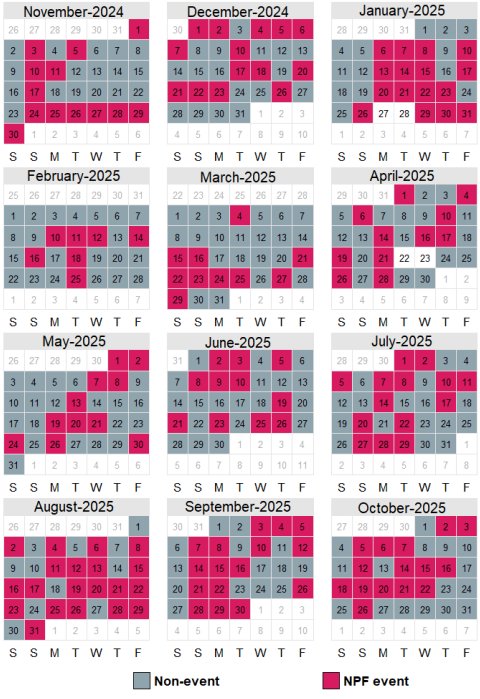


Figure 3. Calendar plot of NPF days. Event days are highlighted in pink and non-event days in gray.

https://doi.org/10.5194/egusphere-2026-7101
Preprint. Discussion started: 20 November 2026
© Author(s) 2026. CC BY 4.0 License.

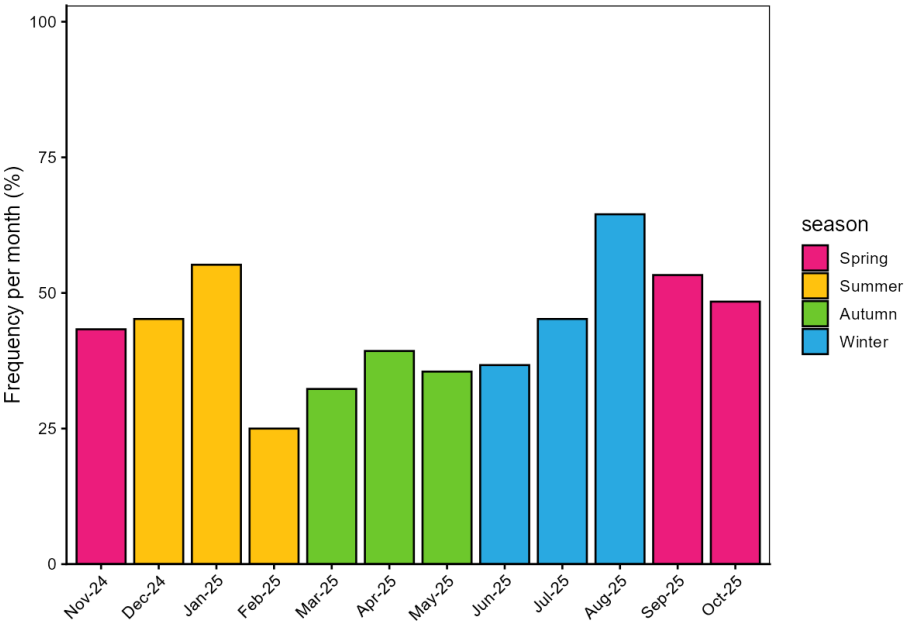


Figure 4. **Frequency of detected events in different seasons and months**

Figure 5 shows the mean diurnal cycle of nucleation-mode particle concentration on NPF event days, and non-event days detected in this study. Between 00:00 and 05:59 LT, the mean nucleation mode concentration was the same on event and non-event days. During the morning rush hours (i.e., 06:00 – 09:59 LT), the concentration on both day types increased, with mean values of 4.53×10^3 cm^{-3} and 3.65×10^3 cm^{-3}, respectively. This minor difference suggests that PNC during these hours is mainly influenced by traffic emissions. After the morning rush hours, when NPF events have previously been reported (Guo et al., 2008), PNC rose sharply from around 10:00 LT, peaking at noon. Between 10:00 and 12:00 LT on event days, the average PNC reached 1.14×10^4 cm^{-3}, which was 2.7 times the concentration observed on non-event days during the same period (4.26×10^3 cm^{-3}). This pattern is consistent with observations from studies conducted in different parts of the world, which reported that NPF activity most frequently peaks around noon. Similar results have been documented in cities such as Xi'an, China (Peng et al., 2017), and across various European urban environments (Hofman et al., 2016), highlighting the role of solar radiation in driving photochemical reactions and enhancing particle formation. In Brisbane, Cheung et al. (2011) reported that PNC increased with solar radiation, which peaks around midday, indicating the role of photochemistry in NPF. It has been shown that NPF is most likely to occur at midday and in the early afternoon, when solar radiation peaks, and less likely in the early morning and late afternoon (Hofman et al., 2016). Overall, because the nucleation mode concentration did not differ notably between event and non-event days during the morning traffic hours, the midday peak on event days is likely related to secondary particles.

https://doi.org/10.5194/egusphere-2026-7101
Preprint. Discussion started: 20 November 2026
© Author(s) 2026. CC BY 4.0 License.

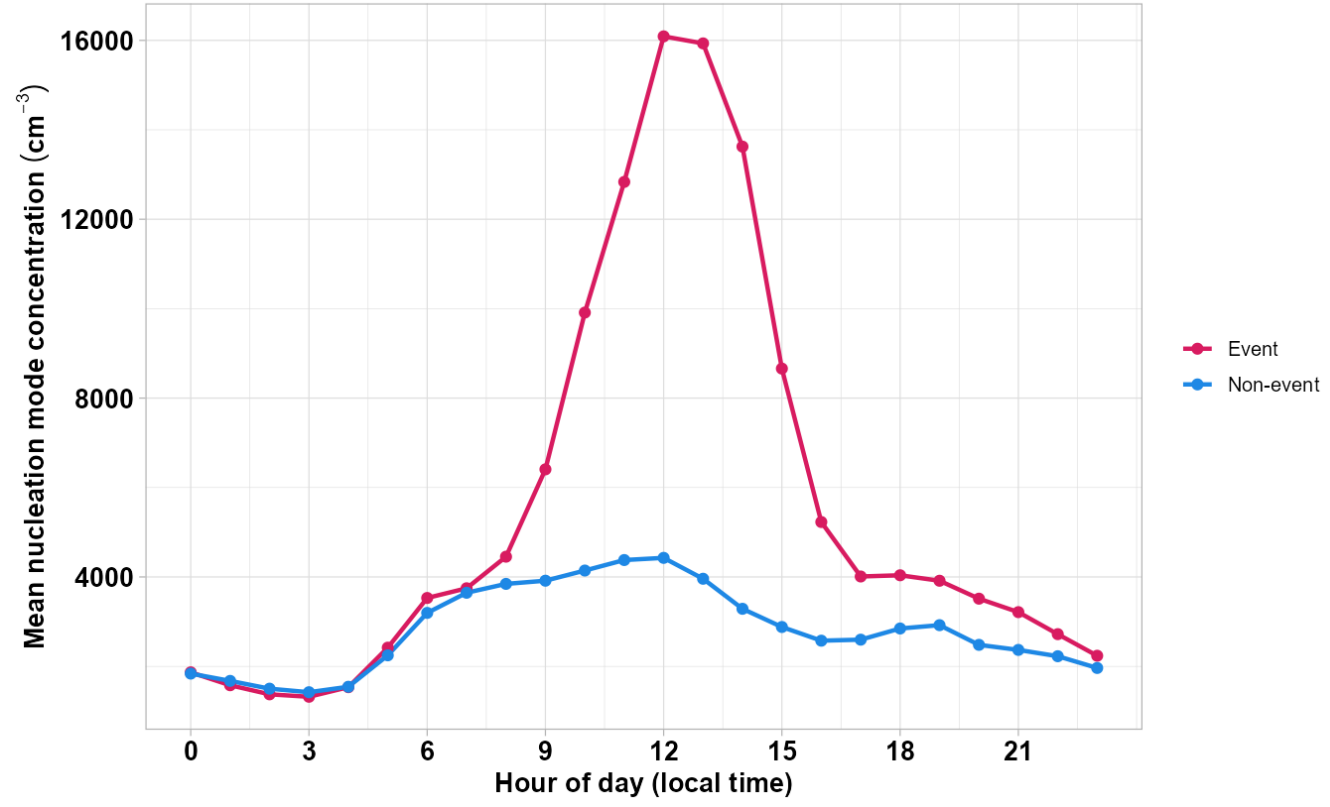


Figure 5. Mean diurnal nucleation-mode particle concentration on NPF event days compared to non-event days, total PNC (cm^{-3}) is displayed in black; particles ≥21 nm and particles <21 nm is shown in blue and pink, respectively.

3.2 Trends of NPF events, PNC, and nucleation mode particles

In this section, two example representative days from this study are examined: an event day on 11 February 2025 (Fig. 6a) and a non-event day on 13 February 2025 (Fig. 6b).

On the event day, two events were identified at 12:00 and 15:30 LT (Fig. 6a). Between 00:00 and 05:00 LT, total PNC remained low, with a mean (median; min-max) of 8.3×10^3 (8.4×10^3; 2.6×10^3, 2×10^4) cm^{-3}. During this period, the average of particles was 29 (28; 19 – 40) nm.

From 06:00 to 09:59 LT, PNC increased, reaching a mean of 1.28×10^4 (1.26×10^4; 8.0×10^3–2.2×10^4) cm^{-3} with an average particle size of 29 (28; 24-45) nm. This suggests that traffic emissions were the main source of particles, as traffic emissions typically show two particle size fractions: primary nucleation-mode particles (<30 nm), and larger particles in the 30–500 nm

https://doi.org/10.5194/egusphere-2026-7101
Preprint. Discussion started: 20 November 2026
© Author(s) 2026. CC BY 4.0 License.

range (Morawska et al., 2008). After 10:00 LT, a nucleation burst occurred, and the mean total PNC between 10:00 and 12:59 LT was 8.5×10^4 (9.4×10^4; 1.4×10^4 - 1.35×10^5) cm^{-3}. As a result, nucleation-mode particles became dominant, with an average particle size of 18 (19; 15-31) nm, indicating freshly formed particles and suggesting an NPF event.

During the second event (15:30-17:00 LT), the mean PNC of 3.2×10^4 cm^{-3} (3.06×10^4 cm^{-3}; 7.2×10^3 cm^{-3} - 7.8×10^4 cm^{-3}) with an average particle size of 17.8 nm (17 nm; 16–26 nm). After 17:00 LT, the nucleation mode disappeared, and particle size grew from 22 to 44 nm, which is comparable to previous studies (Cheung et al., 2011; Pushpawela et al., 2018a). After 18:00 LT, the nucleation-mode reappeared, but Aitken mode was dominant. This pattern is characteristic of the evening rush hours. As on the event day, PNC on the non-event day (Fig. 6b) remained relatively stable during the early morning, with a mean of 3.6×10^3 cm^{-3} (2.5×10^3 cm^{-3}; 1.0×10^3 cm^{-3} - 1.22×10^4 cm^{-3}). During this period, the Aitken mode was dominant, with a mean particle size of 36.8 nm (36 nm; 21-64nm). Between 5:00–9:59 LT, PNC increased because of morning rush hours, with a mean of 1.27×10^4 cm^{-3} (1.23×10^4 cm^{-3}; 5.6×10^3 cm^{-3} - 3.2×10^4 cm^{-3}). During this period, the mean particle size decreased to 25.3 nm (25 nm; 20-39 nm), indicating a contribution of primary particles from morning rush hours emissions, although the Aitken mode remained dominant. After the traffic hours, PNC decreased for the rest of the day, with a mean of 3.8×10^3 cm^{-3} (2.9×10^3 cm^{-3}; 8.2×10^2 cm^{-3} - 1.7×10^4 cm^{-3}), while particle size increased, with a mean of 31 nm. Compared with the event day, this observation further supports the conclusion that the proposed method accurately identified the nucleation burst.

https://doi.org/10.5194/egusphere-2026-7101
Preprint. Discussion started: 20 November 2026
© Author(s) 2026. CC BY 4.0 License.

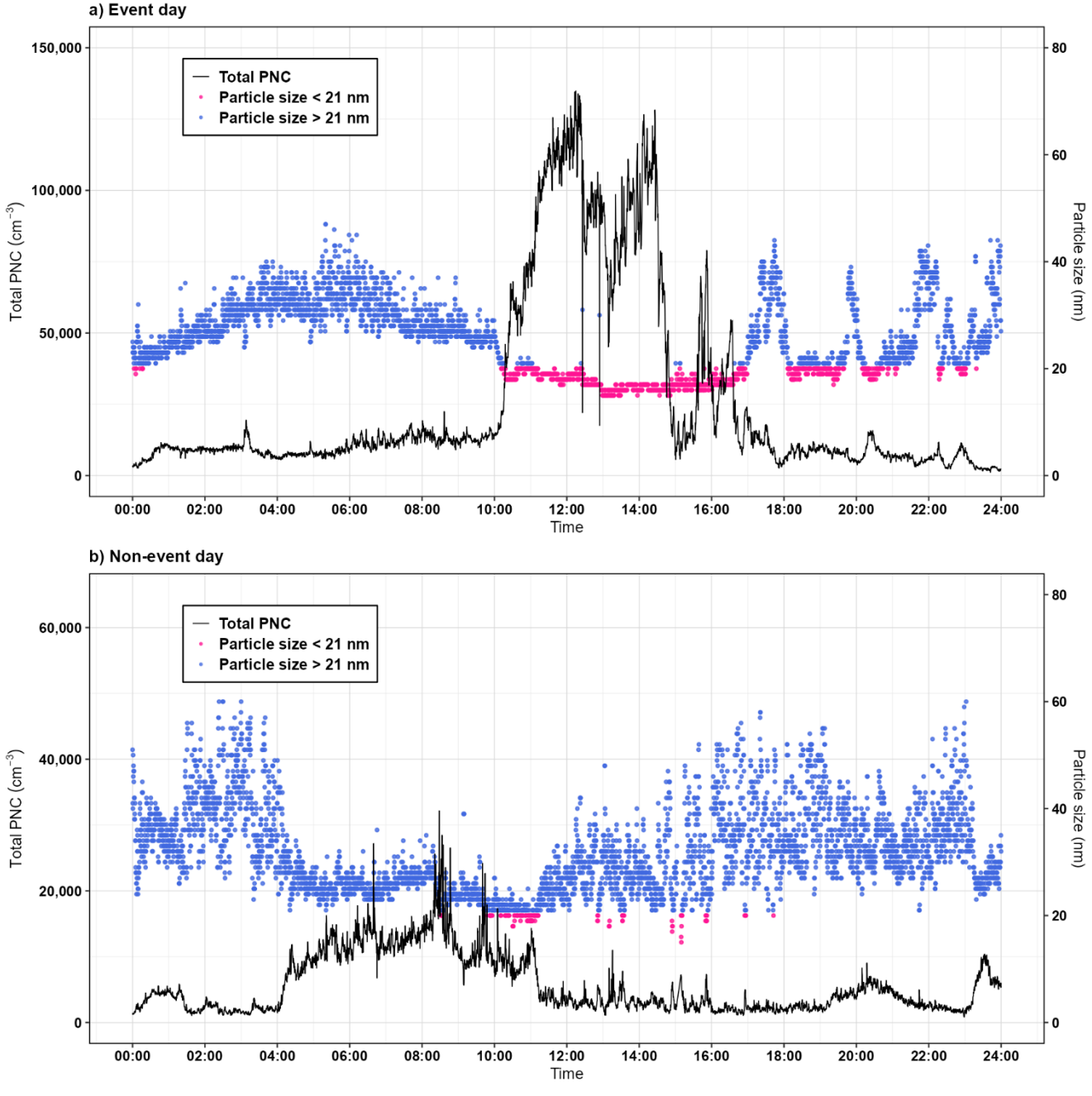


Figure 6. Dual-axis variation of total PNC and particle size in this study during (a) an NPF day (11 February 2025) and (b) a non-event day (13 February 2025).

265 Next, we examined particle concentrations and sizes during five different time windows on these two days. Figure 7 shows the relationship between PNC and particle diameter on the NPF event (a) and the non-event day (b). In urban environments, nucleation-mode particles usually show two traffic-related peaks during the morning and evening rush hours. During NPF

https://doi.org/10.5194/egusphere-2026-7101
Preprint. Discussion started: 20 November 2026
© Author(s) 2026. CC BY 4.0 License.

events, however, an additional sharp nucleation peak often appears around noon, when photochemical activity is strongest, resulting in three peaks. Thus, we considered five time windows: morning (00:00–09:59 LT), midday (10:00–14:59 LT), afternoon (15:00-17:30 LT), evening (17:31-19:59 LT), and night (20:00-23:59 LT). As shown by blue dots (Fig. 7a and b), during the morning rush hours, most particles were in the Aitken mode (i.e., 21 nm-100 nm), with a peak concentration of around 3.0×10^4 cm^{-3} for both days. Traffic-related particles typically show two dominant modes, peaking at around 30–35 nm for spark-ignition vehicles and 60–80 nm for diesel vehicles (Hopke et al., 2022). As the day progressed into the midday period under strong solar radiation, a sharp nucleation mode appeared (pink triangles in Fig. 7a), marked by a sharp increase in PNC and a shift toward smaller particle sizes, both of which are clear signatures of nucleation bursts. In contrast, on the non-event day, the particles did not show a clear temporal partitioning of the nucleation mode (Fig. 7b). Throughout the day, particles <21 nm remained with a relatively narrow concentration range mostly during the midday period, without the long-tail structure of a nucleation bursts as observed on event days.

In the afternoon, another nucleation-mode peak (orange circles, Fig. 7a) was observed, corresponding to the second event, which was weaker than the first event. On the non-event days, by contrast, most particles during the morning, evening, and night window were Aitken mode range (21–60 nm), and only morning window showed high PNC, which could be related to the traffic emissions. In general, on the event day nucleation mode became the dominant size fraction and was present for around 7 h, between 10:00 and 17:00 LT, and then disappeared after 17:00 LT as particles grew to larger particles. Overall, on the event day, these trends show a temporal partitioning of particle sizes, with a sharp midday nucleation burst, providing evidence that supports the predictions of the proposed method.

https://doi.org/10.5194/egusphere-2026-7101
Preprint. Discussion started: 20 November 2026
© Author(s) 2026. CC BY 4.0 License.

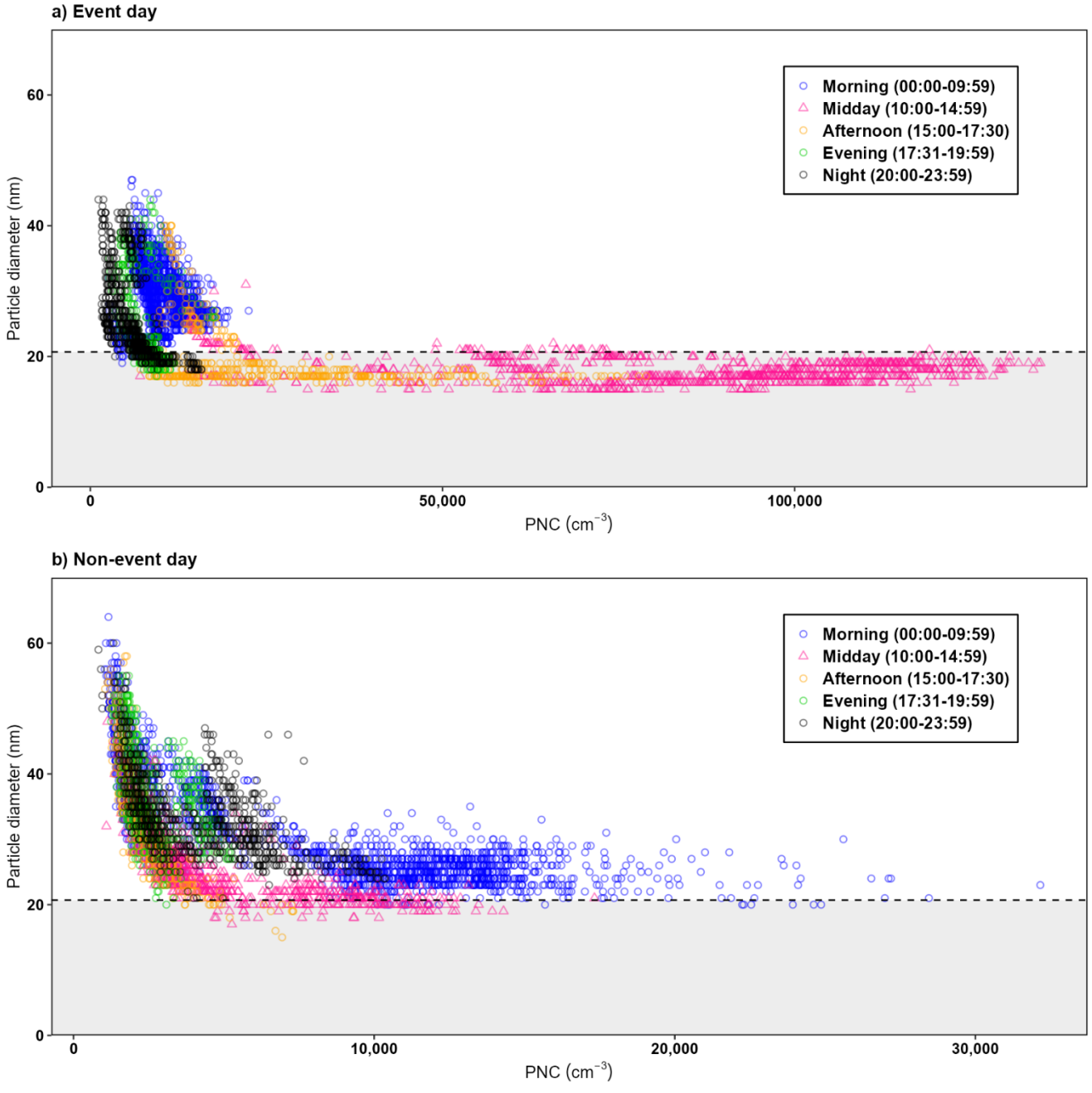


Figure 7. Variation of PNC and particle size observed in this study during (a) an NPF day (11 February 2025) and (b) a non-event day (13 February 2025). Particle sizes (geometric mean diameter) are shown on the left y-axis, while total PNC values shown on the x-axis. The dashed line separates nucleation mode particle from larger particles.

https://doi.org/10.5194/egusphere-2026-7101
Preprint. Discussion started: 20 November 2026
© Author(s) 2026. CC BY 4.0 License.

4 Conclusions

Using a 12-month, 24 h continuous measurement campaign in an urban area, this study proposed and tested a method for identifying NPF with the P2Pro, a lower-cost, simpler, and portable monitor. An event was identified when three conditions were met: (1) the 30-minute average PNC exceeded 2.0×10^4 cm^{-3}, (2) the nucleation mode contribution was more than 50 % of total PNC, and (3) event were separated by at least 3 h. The threshold was selected by comparing the resulting event frequency with those of previous NAIS studies in the same area, and to ensure that nucleation bursts were captured while the contribution of primary nucleation mode particles was excluded. The results showed that NPF days occurred on 158 days (44 % of the measurement period), which was comparable with the frequencies of 37-45% reported by previous NAIS studies at the same location.

The main limitation of the P2Pro is its coarse size resolution. With only eight size channels and a lower size limit of about 8 nm, the instrument cannot capture the earliest stages of nucleation or resolve particle growth in detail, and weak events may therefore be missed or detected later than with an NAIS. In addition, the threshold of 2×10^4 cm^{-3} was derived at a single urban site and may need to be adjusted for locations with different background concentrations. Despite these limitations, the criteria developed in this study produced an NPF frequency comparable with that of NAIS measurements at the same site. This shows that such an instrument can be used to detect NPF where continuous, long-term, and large-scale monitoring of PNC and PNSD with reference instruments is not practical.

Data availability

The data of this paper are available upon request to Lidia Morawska (l.morawska@qut.edu.au).

Author contributions

AJ: Conceptualization, Methodology, Data Curation, Formal analysis, Investigation, Visualization, Writing– Original Draft, Writing– Review and Editing. RJ: Supervision, Conceptualization, Methodology, Data Curation, Formal analysis, Investigation, Visualization, Writing– Review and Editing. AJC: Methodology, Writing– Review and Editing. LM: Supervision, Founding acquisition, Resources, Conceptualization, Project administration, Writing– Review and Editing.

Competing interests

The authors declare that they have no conflict of interest.

https://doi.org/10.5194/egusphere-2026-7101
Preprint. Discussion started: 20 November 2026
© Author(s) 2026. CC BY 4.0 License.

Acknowledgements

This paper was supported by the ARC Training Centre for Advanced Building Systems Against Airborne Infection Transmission (Thrive) (IC220100012).

References

Birmili, W. and Wiedensohler, A.: New particle formation in the continental boundary layer: Meteorological and gas phase parameter influence, Geophys. Res. Lett., 27, 3325–3328, https://doi.org/10.1029/1999GL011221, 2000.

Bischof, O. F., Burtscher, H., and Fierz, M.: Metrology of Nanoparticles, Chimia, 80, 13–20, https://doi.org/10.2533/chimia.2026.13, 2026.

Buenrostro Mazon, S., Riipinen, I., Schultz, D. M., Valtanen, M., Dal Maso, M., Sogacheva, L., Junninen, H., Nieminen, T., Kerminen, V.-M., and Kulmala, M.: Classifying previously undefined days from eleven years of aerosol-particle-size distribution data from the SMEAR II station, Hyytiälä, Finland, Atmos. Chem. Phys., 9, 667–676, https://doi.org/10.5194/acp-9-667-2009, 2009.

Cheung, H. C., Morawska, L., and Ristovski, Z. D.: Observation of new particle formation in subtropical urban environment, Atmos. Chem. Phys., 11, 3823–3833, https://doi.org/10.5194/acp-11-3823-2011, 2011.

Covert, D. S., Kapustin, V. N., Quinn, P. K., and Bates, T. S.: New particle formation in the marine boundary layer, J. Geophys. Res.-Atmos., 97, 20581–20589, https://doi.org/10.1029/92JD02074, 1992.

Dada, L., Chellapermal, R., Buenrostro Mazon, S., Paasonen, P., Lampilahti, J., Manninen, H. E., Junninen, H., Petäjä, T., Kerminen, V.-M., and Kulmala, M.: Refined classification and characterization of atmospheric new-particle formation events using air ions, Atmos. Chem. Phys., 18, 17883–17893, https://doi.org/10.5194/acp-18-17883-2018, 2018.

Dal Maso, M., Kulmala, M., Riipinen, I., Wagner, R., Hussein, T., Aalto, P. P., and Lehtinen, K. E. J.: Formation and growth of fresh atmospheric aerosols: eight years of aerosol size distribution data from SMEAR II, Hyytiälä, Finland, Boreal Environ. Res., 10, 323–336, https://doi.org/10.60910/yq6q-vj10, 2005.

de Jesus, A. L., Rahman, M. M., Mazaheri, M., Thompson, H., Knibbs, L. D., Jeong, C.-H., Evans, G., Nei, W., Ding, A., Qiao, L., Li, L., Portin, H. J., Niemi, J. V., Timonen, H. J., Luoma, K., Petäjä, T., Kulmala, M., Kowalski, M., Peters, A., Cyrys, J., Ferrero, L., Manigrasso, M., Avino, P., Buonanno, G., Reche, C., Querol, X., Beddows, D. C. S., Harrison, R. M., Sowlat, M. H., Sioutas, C., and Morawska, L.: Ultrafine particles and $PM_{2.5}$ in the air of cities around the world: Are they representative of each other?, Environ. Int., 129, 118–135, https://doi.org/10.1016/j.envint.2019.05.021, 2019.

Delfino, R. J., Sioutas, C., and Malik, S.: Potential role of ultrafine particles in associations between airborne particle mass and cardiovascular health, Environ. Health Persp., 113, 934–946, https://doi.org/10.1289/ehp.7938, 2005.

https://doi.org/10.5194/egusphere-2026-7101
Preprint. Discussion started: 20 November 2026
© Author(s) 2026. CC BY 4.0 License.



Fierz, M., Meier, D., Steigmeier, P., and Burtscher, H.: Aerosol measurement by induced currents, Aerosol Sci. Tech., 48, 350–357, https://doi.org/10.1080/02786826.2013.875981, 2014.

Garcia-Marlès, M., Lara, R., Reche, C., Pérez, N., Tobías, A., Savadkoohi, M., Beddows, D., Salma, I., Vörösmarty, M., Weidinger, T., Hueglin, C., Mihalopoulos, N., Grivas, G., Kalkavouras, P., Ondráček, J., Zíková, N., Niemi, J. V., Manninen, H. E., Green, D. C., Tremper, A. H., Norman, M., Vratolis, S., Eleftheriadis, K., Gómez-Moreno, F. J., Alonso-Blanco, E., Wiedensohler, A., Weinhold, K., Merkel, M., Bastian, S., Hoffmann, B., Altug, H., Petit, J.-E., Favez, O., Dos Santos, S. M., Putaud, J.-P., Dinoi, A., Contini, D., Timonen, H., Lampilahti, J., Petäjä, T., Pandolfi, M., Hopke, P. K., Harrison, R. M., Alastuey, A., and Querol, X.: Inter-annual trends of ultrafine particles in urban Europe, Environ. Int., 185, 108510, https://doi.org/10.1016/j.envint.2024.108510, 2024a.

Garcia-Marlès, M., Lara, R., Reche, C., Pérez, N., Tobías, A., Savadkoohi, M., Beddows, D., Salma, I., Vörösmarty, M., Weidinger, T., Hueglin, C., Mihalopoulos, N., Grivas, G., Kalkavouras, P., Ondráček, J., Zíková, N., Niemi, J. V., Manninen, H. E., Green, D. C., Tremper, A. H., Norman, M., Vratolis, S., Diapouli, E., Eleftheriadis, K., Gómez-Moreno, F. J., Alonso-Blanco, E., Wiedensohler, A., Weinhold, K., Merkel, M., Bastian, S., Hoffmann, B., Altug, H., Petit, J.-E., Acharja, P., Favez, O., Dos Santos, S. M., Putaud, J.-P., Dinoi, A., Contini, D., Casans, A., Casquero-Vera, J. A., Crumeyrolle, S., Bourrianne, E., Van Poppel, M., Dreesen, F. E., Harni, S., Timonen, H., Lampilahti, J., Petäjä, T., Pandolfi, M., Hopke, P. K., Harrison, R. M., Alastuey, A., and Querol, X.: Source apportionment of ultrafine particles in urban Europe, Environ. Int., 194, 109149, https://doi.org/10.1016/j.envint.2024.109149, 2024b.

Guo, H., Ding, A., Morawska, L., He, C., Ayoko, G., Li, Y.-S., and Hung, W.-T.: Size distribution and new particle formation in subtropical eastern Australia, Environ. Chem., 5, 382–390, https://doi.org/10.1071/EN08058, 2008.

Hofman, J., Staelens, J., Cordell, R., Stroobants, C., Zikova, N., Hama, S. M. L., Wyche, K. P., Kos, G. P. A., Van Der Zee, S., Smallbone, K. L., Weijers, E. P., Monks, P. S., and Roekens, E.: Ultrafine particles in four European urban environments: Results from a new continuous long-term monitoring network, Atmos. Environ., 136, 68–81, https://doi.org/10.1016/j.atmosenv.2016.04.010, 2016.

Holmes, N. S.: A review of particle formation events and growth in the atmosphere in the various environments and discussion of mechanistic implications, Atmos. Environ., 41, 2183–2201, https://doi.org/10.1016/j.atmosenv.2006.10.058, 2007.

Hopke, P. K., Feng, Y., and Dai, Q.: Source apportionment of particle number concentrations: A global review, Sci. Total Environ., 819, 153104, https://doi.org/10.1016/j.scitotenv.2022.153104, 2022.

Jayaratne, R., Pushpawela, B., and Morawska, L.: Temporal evolution of charged and neutral nanoparticle concentrations during atmospheric new particle formation events and its implications for ion-induced nucleation, Front. Env. Sci. Eng., 10, 13, https://doi.org/10.1007/s11783-016-0862-x, 2016.

Kalkavouras, P., Grivas, G., Stavroulas, I., Petrinoli, K., Bougiatioti, A., Liakakou, E., Gerasopoulos, E., and Mihalopoulos, N.: Source apportionment of fine and ultrafine particle number concentrations in a major city of the Eastern Mediterranean, Sci. Total Environ., 915, 170042, https://doi.org/10.1016/j.scitotenv.2024.170042, 2024.

https://doi.org/10.5194/egusphere-2026-7101
Preprint. Discussion started: 20 November 2026
© Author(s) 2026. CC BY 4.0 License.

Kulmala, M.: Importance of new particle formation for climate and air quality, ACS EST Air, 2, 710–712, https://doi.org/10.1021/acsestair.5c00095, 2025.

Kulmala, M., Vehkamäki, H., Petäjä, T., Dal Maso, M., Lauri, A., Kerminen, V.-M., Birmili, W., and McMurry, P. H.: Formation and growth rates of ultrafine atmospheric particles: a review of observations, J. Aerosol Sci., 35, 143–176, https://doi.org/10.1016/j.jaerosci.2003.10.003, 2004.

Lachowicz, J. I. and Gać, P.: Short-term and long-term effects of inhaled ultrafine particles on blood markers of cardiovascular diseases: a systematic review and meta-analysis, J. Clin. Med., 14, 2846, https://doi.org/10.3390/jcm14082846, 2025.

Lee, H., Cho, H., Yoon, Y. J., Kim, J., Lee, B. Y., and Park, K.: Comparison of new particle formation events in urban, agricultural, and arctic environments, Atmos. Environ., 333, 120634, https://doi.org/10.1016/j.atmosenv.2024.120634, 2024.

Lehtipalo, K., Nieminen, T., Schobesberger, S., Ehn, M., Kulmala, M., and Kerminen, V.-M.: How the understanding of atmospheric new particle formation has evolved along with the development of measurement and analysis methods, J. Aerosol Sci., 184, 106494, https://doi.org/10.1016/j.jaerosci.2024.106494, 2025.

Maes, J., Bezantakos, S., Kavabata, L. K., Biskos, G., and Dedoussi, I. C.: Aircraft emissions of ultrafine particles characterized by real-world near runway measurements, npj Clim. Atmos. Sci., 8, 232, https://doi.org/10.1038/s41612-025-01095-9, 2025.

Mäkelä, J. M., Aalto, P., Jokinen, V., Pohja, T., Nissinen, A., Palmroth, S., Markkanen, T., Seitsonen, K., Lihavainen, H., and Kulmala, M.: Observations of ultrafine aerosol particle formation and growth in boreal forest, Geophys. Res. Lett., 24, 1219–1222, https://doi.org/10.1029/97GL00920, 1997.

Mejía, J. F. and Morawska, L.: An investigation of nucleation events in a coastal urban environment in the Southern Hemisphere, Atmos. Chem. Phys., 9, 7877–7888, https://doi.org/10.5194/acp-9-7877-2009, 2009.

Morawska, L., Ristovski, Z., Jayaratne, E. R., Keogh, D. U., and Ling, X.: Ambient nano and ultrafine particles from motor vehicle emissions: Characteristics, ambient processing and implications on human exposure, Atmos. Environ., 42, 8113–8138, https://doi.org/10.1016/j.atmosenv.2008.07.050, 2008.

Morawska, L., Jayaratne, R., He, C., and Ristovski, Z.: Frequency of new particle formation in Brisbane over the years, 21st International Conference on Nucleation and Atmospheric Aerosols (ICNAA 2023), Brisbane, Australia, 26–30 June 2023, 2023.

Naneos: Partector 2 Pro, https://www.naneos.ch/partector2.html (last access: 9 October 2026), 2026.

Peng, Y., Liu, X., Dai, J., Wang, Z., Dong, Z., Dong, Y., Chen, C., Li, X., Zhao, N., and Fan, C.: Aerosol size distribution and new particle formation events in the suburb of Xi'an, northwest China, Atmos. Environ., 153, 194–205, https://doi.org/10.1016/j.atmosenv.2017.01.022, 2017.

Phunthirawuthi, P., He, C., Jayaratne, R., Thompson, H., and Morawska, L.: Long-term changes in Aitken-mode particle number concentration in Brisbane: roles of meteorology, traffic, and biomass burning, Environ. Int., 110514, https://doi.org/10.1016/j.envint.2026.110514, 2026.

https://doi.org/10.5194/egusphere-2026-7101
Preprint. Discussion started: 20 November 2026
© Author(s) 2026. CC BY 4.0 License.



Pushpawela, B., Jayaratne, R., and Morawska, L.: Differentiating between particle formation and growth events in an urban environment, Atmos. Chem. Phys., 18, 11171–11183, https://doi.org/10.5194/acp-18-11171-2018, 2018a.

Pushpawela, B., Jayaratne, R., and Morawska, L.: Temporal distribution and other characteristics of new particle formation events in an urban environment, Environ. Pollut., 233, 552–560, https://doi.org/10.1016/j.envpol.2017.10.102, 2018b.

Ristovski, Z. D., Suni, T., Kulmala, M., Boy, M., Meyer, N. K., Duplissy, J., Turnipseed, A., Morawska, L., and Baltensperger, U.: The role of sulphates and organic vapours in growth of newly formed particles in a eucalypt forest, Atmos. Chem. Phys., 10, 2919–2926, https://doi.org/10.5194/acp-10-2919-2010, 2010.

Salimi, F., Rahman, M. M., Clifford, S., Ristovski, Z., and Morawska, L.: Nocturnal new particle formation events in urban environments, Atmos. Chem. Phys., 17, 521–530, https://doi.org/10.5194/acp-17-521-2017, 2017.

Schraufnagel, D. E.: The health effects of ultrafine particles, Exp. Mol. Med., 52, 311–317, https://doi.org/10.1038/s12276-020-0403-3, 2020.

Stanier, C. O., Khlystov, A. Y., and Pandis, S. N.: Nucleation events during the Pittsburgh Air Quality Study: description and relation to key meteorological, gas phase, and aerosol parameters, Aerosol Sci. Tech., 38, 253–264, https://doi.org/10.1080/02786820390229570, 2004.

Ueda, S., Miura, K., Kawata, R., Furutani, H., Uematsu, M., Omori, Y., and Tanimoto, H.: Number–size distribution of aerosol particles and new particle formation events in tropical and subtropical Pacific Oceans, Atmos. Environ., 142, 324–339, https://doi.org/10.1016/j.atmosenv.2016.07.055, 2016.

Venzac, H., Sellegri, K., Laj, P., Villani, P., Bonasoni, P., Marinoni, A., Cristofanelli, P., Calzolari, F., Fuzzi, S., Decesari, S., Facchini, M.-C., Vuillermoz, E., and Verza, G. P.: High frequency new particle formation in the Himalayas, P. Natl. Acad. Sci. USA, 105, 15666–15671, https://doi.org/10.1073/pnas.0801355105, 2008.

Vu, T. V., Delgado-Saborit, J. M., and Harrison, R. M.: Particle number size distributions from seven major sources and implications for source apportionment studies, Atmos. Environ., 122, 114–132, https://doi.org/10.1016/j.atmosenv.2015.09.027, 2015.

WHO: WHO global air quality guidelines: particulate matter ($PM_{2.5}$ and PM_{10}), ozone, nitrogen dioxide, sulfur dioxide and carbon monoxide, World Health Organization, Geneva, Switzerland, ISBN 978-92-4-003422-8, 2021.

Zhang, R., Khalizov, A., Wang, L., Hu, M., and Xu, W.: Nucleation and growth of nanoparticles in the atmosphere, Chem. Rev., 112, 1957–2011, https://doi.org/10.1021/cr2001756, 2012.